Research paper

Assessment of two cobalt(II) complexes with pincer ligands for the electrocatalytic hydrogen evolution reaction. A comparison of the SNS vs ONS coordination

Mark A.W. Lawrence, Willem Mulder, Michael J. Celestine, Colin D. McMillen, Alvin A. Holder

PII: S0020-1693(19)31588-9
DOI: https://doi.org/10.1016/j.ica.2020.119497
Reference: ICA 119497

To appear in: *Inorganica Chimica Acta*

Received Date: 17 October 2019
Revised Date: 28 January 2020
Accepted Date: 1 February 2020

Please cite this article as: M.A.W. Lawrence, W. Mulder, M.J. Celestine, C.D. McMillen, A.A. Holder, Assessment of two cobalt(II) complexes with pincer ligands for the electrocatalytic hydrogen evolution reaction. A comparison of the SNS vs ONS coordination, *Inorganica Chimica Acta* (2020), doi: https://doi.org/10.1016/j.ica.2020.119497

Assessment of two cobalt(II) complexes with pincer ligands for the electrocatalytic hydrogen evolution reaction. A comparison of the SNS vs ONS coordination

Mark A.W. Lawrence,[1*] Willem Mulder,[1] Michael J. Celestine,[2] Colin D. McMillen,[3] and Alvin A. Holder[2]

[1]Department of Chemistry, The University of the West Indies Mona, Kingston 7, Jamaica
[2]Department of Chemistry and Biochemistry, Old Dominion University, 4541 Hampton Boulevard, Norfolk, VA 23529, U.S.A.
[3]Department of Chemistry, Clemson University, 379 Hunter Laboratories Clemson, SC 29634, U.S.A.

E-mail: mark.lawrence02@uwimona.edu.jm

Abstract

Bis-*N*-(2,5-dimethoxyphenyl)pyridine-2,6-dicarbothioamide (*pdcta*) and *N*-(2,5-dimethoxyphenyl)-6-[(2,5- dimethoxyphenyl)carbamothioyl]pyridine-2-carboxamide (*pcta*) were synthesized from a one pot mixture as pincer ligands. Crystals of *pcta*, grown from $CDCl_3$ were structurally characterized, and found to crystallize in the space group $P2_1/c$. The Co(II) complexes [Co(II)(κ^3-SNS-pdcta)(CH_3CO_2)(H_2O)] (**1**) and [Co(II)(κ^3-ONS-pcta)(CH_3CO_2)(H_2O)]•H_2O (**2**) were prepared from the reaction of *pdcta* and *pcta* and $Co(CH_3CO_2)_2$•$4H_2O$ in ethanol at reflux under argon atmosphere. The identities of **1** and **2** were confirmed from their elemental analyses, ESI MS and a series of spectroscopic measurements. Both complexes displayed electrocatalytic hydrogen evolution with *p*-toluene sulfonic acid monohydrate in the presence and absence of *bpy* or PPh_3 co-ligands. The hydrogen evolution occurred at moderate overpotentials (605-780) mV, with **1** giving better Faradaic efficiencies than **2** under all the conditions explored herein. Thermodynamic estimates, based on the reduction potentials, suggests that the homolytic pathway for the production of hydrogen from the Co^{III}-hydride species generated in the presence of the proton source, is more favourable than the heterolytic pathway in CH_3CN.

Keywords: cobalt(II); SNS/SNO pincer ligand; electrochemistry; hydrogen; co-ligands

1 Introduction

An ever-increasing consumption of fossil fuels has led to the global energy crisis and environmental deterioration, through the effects of global warming [1, 2]. Batteries and electrical energy is considered as one of the most promising alternatives for replacing fossil fuels energy, but current (popular) methods of electricity generation accounts for ca 25% of global greenhouse

gas emissions [3]. Efficient solar-powered conversion systems exploiting inexpensive and robust catalytic materials for the photo- and photo-electro-catalytic water splitting, photovoltaic cells, fuel cells, and usage of waste products (such as CO_2) as chemical fuels are appealing solutions [4]. Thus there is a growing need for the direct generation of molecular hydrogen from water as a result of it being a convenient and clean energy vector, while utilising renewable resources, for example, water and sun light [5-10].

The hydrogen evolution reaction (HER) has been actively studied as the globe seeks viable long-term alternatives to the use of fossil fuels. Hydrogen [6, 7, 9, 10] is a clean, renewable and high-energy-density source, and its production through the reduction of water appears to be a convenient solution for long-term storage and accessibility. Hydrogenases are known to catalyze the (reversible) reduction of protons into molecular hydrogen efficiently in nature. There is a search for catalysts that can facilitate the reduction of protons to hydrogen, while using cheap and Earth abundant metals such as Fe, Ni, Co, and Zn, and this represents an area of current interest [11-29]. Such catalysts include cobaloximes [30, 31], cobalt diimine–dioximes [17, 24], and cobalt dithiolenes [19] to name a few (Figure 1).

Fihri *et al*. [32] reported the first cobaloxime-based photocatalytic system for hydrogen evolution. The complex $[(bpy)_2Ru(L\text{-}pyr)Co(dmgBF_2)_2(OH_2)]^{2+}$ (where L-pyr = (4-pyridine)oxazolo[4,5-f]phenanthroline and $dmgBF_2$ = difluoroboryldimethylglyoximato) harvests photons from the $[Ru(bpy)_3]^{2+}$ moiety and drives electrons to the $[Co(dmgBF_2)_2]$ moiety, which is a hydrogen evolving catalyst. This complex was able to perform around 105 turnovers over 15 hours [32]. The issue with this complex is that it requires UV irradiation and is relatively inactive under visible irradiation ($\lambda > 380$ nm). Fihri *et al.* [14] also synthesized two more complexes to get past the issue of the first complex. The two complexes, $[(dmphen)_2Ru(L\text{-}pyr)Co(dmgBF_2)_2(OH_2)](PF_6)_2$ and $[(ppy)_2Ir(L\text{-}pyr)Co(dmgBF_2)_2(OH_2)]PF_6$, were comparable or better than platinum-based systems [14]. The complexes were able to produce hydrogen under visible irradiation with a higher number of turnovers, up to 273 turnovers.

Cropek *et al.* [33] reported the effects of ligand structure on the photocatalytic production of hydrogen in acidic media. The complexes used were three mixed metal complexes with a Ru(II) moiety as a photosensitizer and a Co(II) moiety as a catalyst. Photochemical studies were done with the complexes in acetonitrile with *p*-cyanoanilinium tetrafluoroborate as the proton source

and either triethylamine or triethanolamine as the sacrificial electron donor. From the photocatalytic studies, they concluded that the terminal ligand affects the catalyst and its performance, and the sacrificial electron donor affects the amount of hydrogen produced, and the lifespan of the catalyst. One of the complexes, $[Ru(pbt)_2(L\text{-}pyr)Co(dmgBF_2)_2(OH_2)](PF_6)_2$ (where pbt = 2-(2′-pyridyl)benzothiazole), performed better than the other complexes, as this complex was able to produce hydrogen over a 42 hour period with triethylamine as the sacrificial electron donor [33].

Others have reported on hydrogen production from acidic media with cobalt(III) complexes as electrocatalysts. Peng *et al.* [34] reported on a water soluble complex, $[(phen)_2Co(CN)_2]NO_3$, producing hydrogen from both acetic acid and an aqueous buffer. In acetic acid, the complex could produce hydrogen through electro-catalysis with a turnover frequency of 0.0154 mol of H_2 per mole of catalyst. In a neutral aqueous buffer, the turnover frequency was 0.25 mol of H_2 per mole of catalyst. The most plausible mechanism for the production of hydrogen during the catalysis involves the formation of a Co(I) species which reacts with a proton source to form a Co(III)-hydride via oxidative addition, from which hydrogen may be produced via a homolytic or heterolytic pathway [35-37]. The formation and stability of the Co(I) intermediate is thus an important consideration in the development of a suitable (pre-)catalyst for the hydrogen evolution reaction (HER). To this end, various researchers have studied the spectral characteristics of Co(I) species generated via photochemical [38], chemical [39-42], and electrochemical [42-45] reduction methods. Stubbert *et al.* [22] reported that the ligand may also directly aid in the electrocatalytic process of a cobalt bis(iminopyridine) complex, and it was also noted that certain ligands, such as 1,5-diphenylcarbazone, may actually inhibit electrocatalytic behavior, if they can be easily protonated and cause solvolysis [46]. Hickey *et al.* [45] through a series of *N*,*N*-bidentate ligands, also demonstrated that if the ancillary ligand(s) is (are) not bulky enough to minimize disproportionation, the electrocatalytic process can be suppressed and the formation of cobalt metal on the electrode surface prevails.

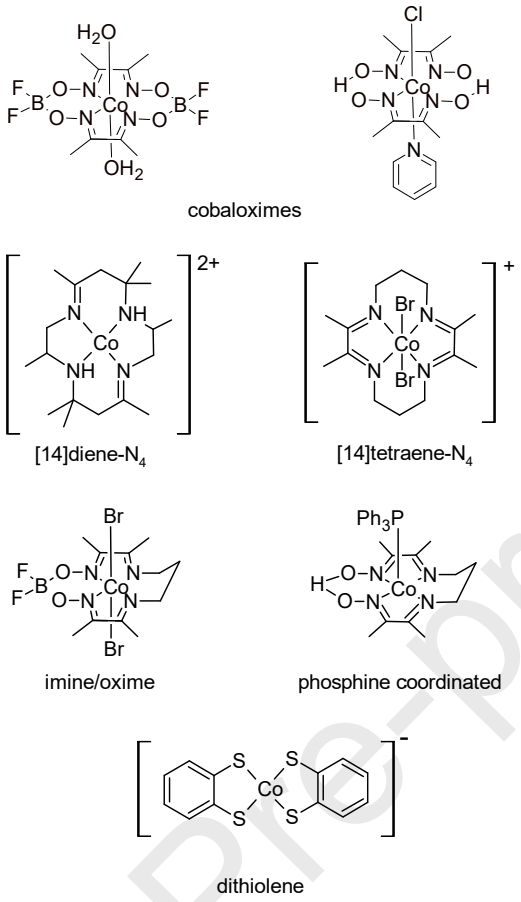

Figure 1. Structural examples of cobalt complexes used in HER.

For many years, pincer complexes of various designs have been applied with varying success in catalytic and electrocatalytic HER [47-49]. Like pincer ligands, thioamide moieties have attracted attention due to their ability to tautomerize upon deprotonation, and coordinate to a variety of transition metals [50-56]. Palladium(II) complexes bearing thioamide pincer ligands of the type 2,6-bis-thioamidophenyl and 2,6-bis-thioamidopyridine have been reported as active catalysts for the Mizoroki-Heck cross-coupling reaction [52], and bis-*N*-(2,5-dimethoxyphenyl)pyridine-2,6-dicarbothioamide (*pdcta*) and 6-(4,7-dimethoxy-2-benzothiazolyl)-*N*-(2,5-dimethoxyphenyl)-2-pyridinecarbothioamide (*pbcta*) have shown potential in HER [57]. Our interest in the electron transfer processes involving transition metal complexes [51, 58-64], as well as the electrocatalytic reduction of protons and small molecules, such CO_2 [41, 42, 65, 66], has led to the development of pincer ligands, bearing sulfur (from thioamides) and nitrogen coordination sites of the types κ^3-SNS and SNN [51, 57]. In this report, we examine the electrocatalytic HER and the effect of substituting a sulfur with and oxygen atom on the same ligand back bone, via a κ^3-SNS and ONS

pincer ligand system; and also the effect of co-ligands 2,2'-bipyridine (*bpy*) and triphenylphosphine (PPh_3) on the voltammetric response of the cobalt complexes *in situ,* on the path to efficient molecular systems for HER.

2 Experimental

All reagents were purchased from commercial sources (BDH and Sigma-Aldrich) and solvents were purchased as HPLC grade and used without further purification. Absorbance measurements were performed on a HP 8453A diode array spectrophotometer. IR spectra were recorded as neat samples using an ATIR accessory on a Bruker Vector 22 FTIR spectrophotometer. NMR spectra were recorded on a Bruker ACE 500 MHz FT spectrometer and the resonances are reported in δ units downfield from TMS as an internal standard or to the residual protons in the incompletely deuterated solvent.

All high resolution ESI MS spectra were acquired via positive electrospray ionization on a Bruker 12 Tesla APEX –Qe FTICR-MS with and Apollo II ion source at the College of Sciences Major Instrument Cluster (COSMIC), Old Dominion University, 143 Oceanography & Physical Sciences Building Norfolk, VA 23529, U.S.A. Samples were dissolved in acetonitrile or 1:1 dichloromethane/acetonitrile, followed by direct injection using a syringe pump with a flow rate of 2 μL s^{-1}. The data was processed using Bruker Daltonics Data Analysis Version 3.4.

All electrochemical experiments were performed on a DigiIvy DY2312 potentiostat, under an argon atmosphere at room temperature. A standard three electrode cell setup was employed, using a glassy carbon working electrode (diameter = 3 mm), a silver wire quasi-reference electrode and a platinum wire as an auxiliary electrode. Ferrocene, which was used as an internal reference showed a reversible wave at +0.48 V in CH_3CN. The ionic strength was maintained at 0.1 M $[^nBu_4N]PF_6$. The solvents used in the electrochemical experiments were dried using standard procedures [67].

Controlled-potential electrolysis (CPE) measurements for the production of hydrogen were conducted at –1.10 and –1.25 V (vs Ag), on unstirred solutions for 20 min in a sealed two-chambered H-cell separated by a fine frit, where one chamber held the working and reference

electrodes in 10 mL of 0.3 mM of complex in 0.1 M [^{n}BuN$_4$]PF$_6$ (supporting electrolyte) with 11 mM *p*-toluenesulfonic acid monohydrate (*p*-TSOH) (as a proton source) and the second chamber held the auxiliary electrode in 5 mL of the solvent with the supporting electrolyte. A glassy carbon plate (contact area ~2 cm × 1 cm × 3 mm) and Pt wire were used as the working and auxiliary electrodes, respectively, with Ag wire as the reference electrode. The solution was purged with Ar for 20 minutes and then sealed under an Ar atmosphere before the start of each electrolysis experiment. The amount of H_2 evolved was calculated based on the charge accumulated from the catalyst solution during CPE minus the charge from the same solution without any catalyst.[68] After electrolysis, 50 μL of the headspace was injected into the gas chromatograph (GC). GC experiments were performed on an HP (Agilent) 5890 series II instrument with an ECD detector (40 ^{o}C isothermal; 1.0 mL min^{-1} flow rate; He carrier gas) [69]. The remainder of the gas in the headspace was analyzed with a PGas-22 H_2 gas detector.

2.1 Semi-Empirical and Density Functional Theory calculations

Density functional theory and semi-empirical calculations were carried out using the GAMESS software package† [70, 71]. The structures were optimized in the gas phase as indicated by the absence of imaginary frequencies in the Hessian, using PM3, and B3LYP methods. The Pople double-eta with the common polarization and diffuse options basis set, 6-31G(d,p) was employed in all DFT calculations. The GAMESS input files were generated using Avogadro [72] version 1.2.0‡, and the output file viewed using the same.

2.2 Preparation of bis-*N*-(2,5-dimethoxyphenyl)pyridine-2,6-dicarbothioamide (pdcta) and *N*-(2,5- dimethoxyphenyl)-6-[(2,5- dimethoxyphenyl)carbamothioyl]pyridine-2-carboxamide (pcta)

High yield of bis-*N*-(2,5-dimethoxyphenyl)pyridine-2,6-dicarbothioamide (*pdcta*) was prepared following the reported procedure [51, 57]. In a 100 cm^3 round bottom flask, bis-*N*-(2,5-

† GAMESS: an open-source general ab initio quantum chemistry package.
https://www.msg.chem.iastate.edu/gamess/index.html
‡ Avogadro: an open-source molecular builder and visualization tool. Version 1.2.0. http://avogadro.cc/

dimethoxyphenyl) pyridine-2,6-dicarboxamide (0.25 g, 0.57 mmol) and 2,4-bis(4-methoxyphenyl)-1,3,2,4-dithiadiphosphetane 2,4-disulfide (Lawesson's reagent (LR); 0.30 g, 0.74 mmol) were suspended in toluene (35 cm^3) and refluxed under argon for 7 h. This mixture was transferred to a 100 cm^3 beaker and evaporated to dryness under a strong stream of air. This crude material was purified by column chromatography (silica) using dichloromethane/hexanes (3:2), followed by ethyl acetate. The dichloromethane/hexanes solvent mixture gave a yellow–orange crystalline product, bis-*N*-(2,5-dimethoxyphenyl)pyridine-2,6-dicarbothioamide, *pdcta* (R_F = 0.24 in dichloromethane/hexanes (3:2); yield = 74 mg (28%), m.p. = 163–165 °C, and the back fraction (from ethyl acetate) gave an orange-yellow crystalline product *N*-(2,5- dimethoxyphenyl)-6-[(2,5-dimethoxyphenyl)carbamothioyl]pyridine-2-carboxamide, *pcta* (R_F = 0.05 in dichloromethane/hexanes (3:2); 119 mg, 46%), mp 140–142 °C. Elemental analysis: Found: C, 60.85; H, 5.10; N, 9.31. Calc. for $C_{23}H_{23}N_3O_5S$: C, 60.91; H, 5.11; N, 9.27%. δ_H ($CDCl_3$) 3.79 (3H, s), 3.83 (3H, s), 3.85 (6H, s), 6.67 (1H, d), 6.79 (1H, d), 6.86 (1H, d), 6.94 (1H, d), 8.09 (1H, t), 8.30 (1H, s), 8.44 (1H, d), 8.95 (1H, d), 9.26 (1H, s), 10.27 (1H, br s, NH), 12.30 (1H br s, NH). δ_C ($CDCl_3$) 55.9, 56.0, 56.1, 56.5, 106.5, 107.1, 109.5, 110.9, 111.1, 111.8, 124.6, 127.6, 127.8, 128.9, 139.1, 143.1, 144.5, 147.9, 151.7, 153.3, 154.0, 161.3, 185.5. Selected ν_{max} (neat)/cm^{-1} 3366 (NH), 3280 (NH), 1689 (amide I), 1599, 1530, 1491, 1443, (pyridyl and aryl), 1220.

2.3 Preparation of [Co(pdcta)(CH_3CO_2)(H_2O)] (1)

In a pressure tube, *pdcta* (30.1 mg, 64 μmol), and $Co(CH_3CO_2)_2 \bullet 4H_2O$ (16.1 mg, 65 μmol) were suspended in EtOH (5 mL). The mixture was sparged with Ar and refluxed for 2.5 h, following which it was concentrated under a strong stream of air. The reaction mixture was filtered; then the residue was washed with cold Et_2O and air dried. Yield = 31 mg (80%). High resolution ESI MS (positive mode) m/z = 604.60336 for the $[Co^{III}(pdcta)(CH_3CO_2)(H_2O)]^+$ and 605.12019 for the $[Co^{II}(pdcta)(CH_3CO_2)(H_2O)]$-$H^+$ species. Elemental analysis: Found: C, 49.27; H, 4.14; N, 6.72. Calc. for $C_{25}H_{27}N_3O_7S_2$: C, 49.67; H, 4.50; N, 6.95%. λ_{max} (DMSO)/nm (ε/M^{-1} cm^{-1}) 283 (19480), 389 (8100) and 493 sh (3500); (CH_3CN)/nm (ε/M^{-1} cm^{-1}) 198 (14250), 281 (4800), 392 (2300), 488 sh (1000). Selected ν_{max} (KBr)/cm^{-1} 3549, 3475 (OH), 3239 (NH), 1619 (C=N).

2.4 Preparation of [Co(pcta)(CH_3CO_2)(H_2O)]•H_2O (2)

In a pressure tube, *pcta* (30.0 mg, 66 μmol), and $Co(CH_3CO_2)_2$•$4H_2O$ (16.5 mg, 66 μmol) were suspended in EtOH (5 mL). The mixture was sparged with Ar and refluxed for 2.5 h, following which it was concentrated under a strong stream of air. The reaction mixture was filtered; then the residue was washed with cold Et_2O and air dried. Yield = 38 mg) (95%). High-resolution ESI MS (positive mode) m/z = 589.10577 for the $[Co^{II}(pcta)(CH_3CO_2)(H_2O)]$-$H^+$ and 588.04567 for the $[Co^{III}(pcta)(CH_3CO_2)(H_2O)]^+$ species. Elemental analysis: Found: C, 49.20; H, 4.35; N, 6.92. Calc. for $C_{25}H_{29}N_3O_9S$: C, 49.51; H, 4.82; N, 6.93%. λ_{max} (DMSO)/nm (ε/M^{-1} cm^{-1}) 270 (12700), 400 and 500 sh (3500 and 1400); (CH_3CN)/nm (ε/M^{-1} cm^{-1}) 201 (17100), 264 (4490), 319 and 478 sh (2514 and 479). Selected ν_{max} (KBr)/cm^{-1} 3443 br (OH), 3380 (NH), 1685 (amide I), 1619 (C=N).

2.5 Voltammograms in the presence of co-ligands PPh_3 and bpy

Stoichiometric amounts of triphenyl phosphine or 2,2'-bipyridine were added to 1.4 mM acetonitrile solutions of **1** or **2** in the supporting electrolyte. The solution was stirred and sparged with Ar for 10-15 minutes following which the voltammograms were acquired.

2.6 X-ray crystallography

A crystal of *pcta* grown from $CDCl_3$, of approximate dimensions 0.06 × 0.16 × 0.21 mm, was used for the X-ray crystallographic analysis. A Bruker D8 Venture diffractometer with Mo Kα radiation (IμS, Incoatec, λ = 0.71073 Å) and a Photon 100 detector were used for the data collection. The structure was solved (intrinsic phasing, SHELXT) and refined (full-matrix least squares on F^2, SHELXL) using the Bruker SHELXTL [73] Software Package. The space group selection of $P2_1/c$ was made based on the systematic absences. All non-hydrogen atoms were refined anisotropically. Hydrogen atoms attached to carbon atoms were refined in geometrically optimized positions using riding models. The hydrogen atoms attached to nitrogen atoms were identified from the difference electron density map and fully refined. Details of data collection and structural solution for *pcta* are provided in the supporting crystallographic files (CCDC deposition number 1957918), and Table 1.

3 Results and Discussion

3.1 Synthesis and characterization

3.1.1 Ligands *pcta* and *pdcta*

The synthesis of the asymmetric pincer ligand *pcta* was affected by modifying the reaction time and ratio of Lawessons's reagent in the protocol used to prepare *pdcta* (Scheme 1). Both ligands can be prepared from a one-pot mixture (see experimental section) as they are each other's by-product in the thionation employing Lawessons's reagent. Consequently, the yield of *pdcta* is determined by the ratio of Lawessons's reagent and reaction time. In the ^{1}H and ^{13}C NMR spectra of *pcta*, the amide and thioamide protons and carbonyl groups are clearly resolved (Fig. S1), and this can be used to assess the quality of the purification process. In the ^{1}H NMR spectrum measured in $CDCl_3$, the amide proton of *pcta* is observed as a singlet at 10.27 ppm, whereas the thioamide proton in this molecule is observed at 12.30 ppm. In *pdcta* the thioamide protons are observed as a singlet (integrating for 2 H) at 12.84 ppm. In the ^{13}C NMR spectra, the amide and thioamide of *pcta* are observed at 161.3 and 185.5, respectively, whereas in *pdcta*, the thioamide is observed at 184.3 ppm. The asymmetry of the molecule also resulted in the splitting of the methoxy protons.

The formulation of *pcta* was further confirmed from the elemental analysis and X-ray crystallography (Table 1). Crystals of *pcta* grown from $CDCl_3$ were characterized by single crystal X-ray diffraction, resulting in a well-refined structure in space group $P2_1/c$ (Fig. 2). The bond lengths and angles are within the normal ranges, and are very similar to the analogous *pdcta* [51]. The two aryl rings are non-coplanar with one another, as the ring containing the thioamide moiety is twisted out of the plane of the pyridyl and aryl ring with amide moiety by 31.83°. Weak C-H···O intermolecular interactions from the C14 and C22 methyl groups (C14-H14B···O3 = 3.446(3) Å, 175.9° and C22-H22B···O1 = 3.317(3) Å, 158.4°) may contribute to the conformation of the molecule, and provide packing interactions along the *a*- and *b*-axes. Stacking interactions between the pi systems of neighbouring molecules (shortest C···C distance = 3.305 Å) provide additional stability. Intramolecular N-H···O and N-H···N interactions (D-H···A = 2.575(2)-2.705(2) Å) may also contribute to the conformation of the molecule.

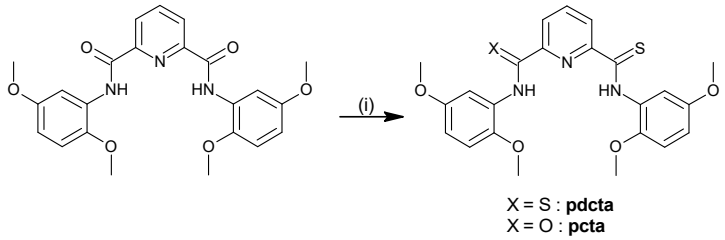

Scheme 1. Preparation of pyridylcarbo(thio)amides. *Reagents and conditions*: (i) Lawesson's reagent, toluene, reflux.

Table 1. Crystal data and structure refinement for *pcta*.

Identification code	*pcta*
Chemical formula	$C_{23}H_{23}N_3O_5S$
Formula weight	453.50 g/mol
Temperature	173(2) K
Wavelength	0.71073 Å
Crystal size	0.06 × 0.16 × 0.21 mm
Crystal system, space group	Monoclinic, $P2_1/c$
Unit cell dimensions	a = 17.0733(17) Å
	b = 8.5106(8) Å
	c = 16.8262(15) Å
	β = 117.271(3)°
Volume (Å^3)	2173.2(4)
Z, Calculated density (g cm^{-3})	4, 1.386
Absorption coefficient (mm^{-1})	0.190
F(000)	952
θ range for data collection (°)	2.68 to 26.39°
Range of *h*, *k*, *l*	–21/21, –10/10, –21/20
Reflections collected/unique	50314/4448 [R(int) = 0.0716]
Max. and min. transmission	1.0000 and 0.9277
Data/restraints/parameters	4448/2/301
Goodness-of-fit on F^2	1.048
Final *R* indices [3484 data; $I>2\sigma(I)$]	R_1 = 0.0471, wR_2 = 0.1107
R indices (all data)	R_1 = 0.0661, wR_2 = 0.1199
Largest diff. peak and hole (eÅ^{-3})	0.386 and -0.430
CCDC no.	1957918

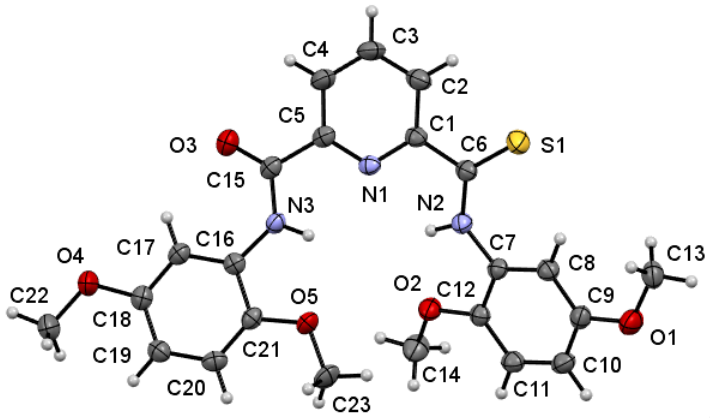

Figure 2. Structure of *pcta*, shown as 50 % probability ellipsoids. Selected bond lengths (Å): C6-S1 = 1.659(2), C6-N2 = 1.343(3), C7-N2 = 1.408(3), C1-N1 = 1.343(3), C5-N1 = 1.344(2), C15-N3 = 1.352(3), C16-N3 = 1.402(3), C15-O3 = 1.236(2).

3.1.2 Complexes 1 and 2

The synthesis of cobalt(II) complexes **1** and **2**, was affected following the general procedure illustrated in Scheme 2, and the species were isolated as dark brown solids in yields of 80 and 95%, respectively. The spectroscopic and elemental analyses, along with the ESI-MS are consistent with the proposed formulations. In the IR spectra, a broad band in the region associated with water was observed in the spectra of **1** and **2**, indicating the presence of water in the structure of the solid. In **2**, the reduction in the wavenumber of the amide I band is suggestive of a pseudo-coordination between the metal centre and the oxygen of the amide moiety. In the paramagnetic ^{1}H NMR spectra of both **1** and **2** (Fig. S2 and S3), the pyridyl ring is deshielded by the paramagnetic envelope of the Co(II), however, the aryl rings which are further away from the influence of the Co(II) are less affected and are observed in the diamagnetic region. In both complexes NH proton is observed above 10 ppm, which is consistent with the formulation proposed in scheme 2.

The presence of exchangeable solvent in the coordination sphere suggests there is most likely an exchange of the water ligand with the solvent upon dissolution. This can also be inferred from the effect of the solvent on the molar absorptivity values as well as its effect on the profile of the electronic spectra of the complexes (Figs. S5 and S6). The UV-visible spectra are dominated by

low energy transitions in the visible region corresponding to Co(II) *d-d* transitions which merges into MLCT and π-π* transitions of the ligands in the UV regions in the spectra of both species. The features of the electronic spectra are consistent with a low spin Co(II) complex [33].

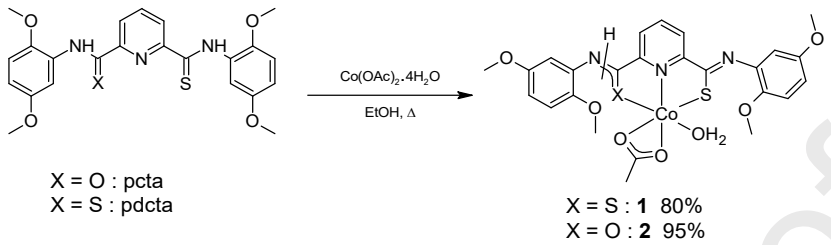

Scheme 2. Preparation of the Co pincer complexes.

3.2 Voltammetric properties of *pcta* and complexes 1 and 2

Density functional theory calculations analysing the molecular orbitals of *pcta* (Fig. S7) revealed that the HOMO and LUMO+1 are centred on the amidic moiety whereas the LUMO and HOMO-1 are centred on the thioamide moiety. Further assessment of the iminothiol tautomerized molecule of *pcta* (which is the protonated form of the coordinated molecule) indicated that the HOMO also resided on the amide portion of the molecule, the LUMO on the iminothiol and the LUMO+1 switches also back to the amide moiety. From the calculations, the features of the redox chemistry of either the thioamide or iminothiol tautomer is thus expected to be similar, with differences occurring in the redox potentials. Similar assessment of *pdcta* revealed that the thioamide moiety is dominant in its redox chemistry [57]. In the cyclic and square wave voltammograms of *pdcta*, the characteristic feature was indeed the reduction and oxidation of the thioamide moiety [57]. The reduction followed the pattern of: (i) an irreversible reduction to yield the thienyl radical anion, followed by (ii) a second irreversible reduction to produce the thienyl dianion; and with (iii) subsequent reductions occurring on the aromatic rings [57]. Similarly, the initial phase of the voltammograms of *pcta* (Fig. S8) is characterized by the reduction of the thiomaide moiety which is more accessible than the amide moiety however, the on the anodic side the amide oxidation partially overlaps that of the thioamide. Similar to another pincer ligand *pbcta* (where *pbcta* = 6-(4,7-dimethoxy-2-benzothiazolyl)-*N*-(2,5-dimethoxyphenyl)-2-pyridinecarbothioamide) [57], the asymmetry of *pcta* renders the first reduction of the thioamide (at $E_{½}$ = –1.16 V vs Ag) reversible, and the second reduction quasi-reversible (at $E_{½}$ = –1.57 V), followed by two closely spaced reductions between E_{pc} = –1.90 to –2.05 V assigned to the amide moiety. The oxidations are

observed at E_{pa} = +1.62 (ca 4 electrons) and +1.8 V. The multi-electron oxidation was also observed for the *pdcta* molecule.

The voltammetric response of **1** and **2** is summarized in Scheme 3. In the voltammograms of the cobalt(II) complexes, an adsorption wave is observed at ca –0.5 V (which disappears on repetitive cycling, Fig. S9). The coordination of *pcta* to Co(II) to produce **2** removes the reduction wave (and also the oxidation wave) associated with the thioamide moiety, and a new quasi-reversible (I_{pa}/I_{pc} = 0.61) wave is observed at $E_{½}$ = –1.22 V which is ca 60 mV more negative than the first reduction wave of the ligand (Fig. 3a and b). This new reduction is assigned to the $Co^{2+} \rightarrow Co^{+}$ process in complex **2.** In the cyclic and square wave voltammograms, the $Co^{+} \rightarrow Co^{0}$ reduction is observed as a shoulder at –1.50 V (vs Ag) on the ligand reduction occurring at E_{pc} = –1.68 V. The oxidation of $Co^{2+} \rightarrow Co^{3+}$ is observed at E_{pa} = +1.30 V as a shoulder on the ligand oxidation at E_{pa} = +1.47 V (Fig. 3 and Fig. S10). DFT calculations suggests that the HOMO and LUMO and LUMO+1 of **2** are largely localized the metal centre, with some delocalization across the ligand (Fig. 4), and are thus consistent with the assignments. The delocalization of the orbitals may also be a contributing factor in the quasi-reversibility of the metal reduction observed in the voltammograms. In acetonitrile it is expected that the aqua ligand will be readily substituted by the solvent, and it is also known that the coordination number of Co(I) changes to five, from coordination number six of the Co(II) precursor, which naturally results in the exclusion of a ligand [44]. Furthermore the Co(I) metal centre has a greater affinity for nitrogen based ligands compared to aqua and halogen ligands [16, 44, 74], and it is thus likely that the acetate ligand is excluded. This might be the driving force behind the quasi-reversibility.

The reaction of *pdcta* with Co(II) to produce **1**, resulted in the suppression the thioamide reduction and produced a new quasi-reversible (I_{pa}/I_{pc} = 0.75) reduction wave at $E_{½}$ = –1.08 V. This reduction potential has been ascribed to the $Co^{2+} \rightarrow Co^{+}$ reduction in complex **1**. The second reduction at $E_{½}$ = –1.74 V is tentatively assigned to the $Co^{+} \rightarrow Co^{0}$ based on its quasi-reversible nature as well as the 1:1 cathodic current when compared to the first reduction wave (Fig. S8). On the oxidation side, the $Co^{2+} \rightarrow Co^{3+}$ is observed at E_{pa} = +1.05 V, also as a shoulder on a second oxidation at E_{pa} = +1.33 V, which is ligand-based. Like **2**, DFT calculations suggests that the HOMO, LUMO, and LUMO+1 may also involve the ligand orbitals. The voltammetric response of the ligands when coordinated to the cobalt metal is similar in nature to those reported for the Pd(II) systems

containing *pbcta* and *pdcta* [51, 57], and consequently these effects induced by the metal ion on the reduction potentials of the ligands are in accord with the proposed structure in which the ligand exists in its anionic (tautomerized, N=C–S$^-$) form. In both complexes **1** and **2**, scan rate variations around $E_{pc,1}$ and $E_{pc,2}$ revealed that the peak currents increase linearly with the square root of the scan rate, which is consistent with electrochemical processes that are diffusion controlled.

Reduction	Oxidation
$Co^{II}L + e^- \rightarrow Co^{I}L$	$Co^{II}L - e^- \rightarrow Co^{III}L$
$Co^{I}L + e^- \rightarrow Co^{0}L$	$Co^{III}L - 2e^- \rightarrow Co^{III}L^{2+}$
$Co^{0}L + 2e^- \rightarrow Co^{0}L^{2-}$	

Scheme 3. Summary of the voltammetric responses of **1** and **2** in CH_3CN.

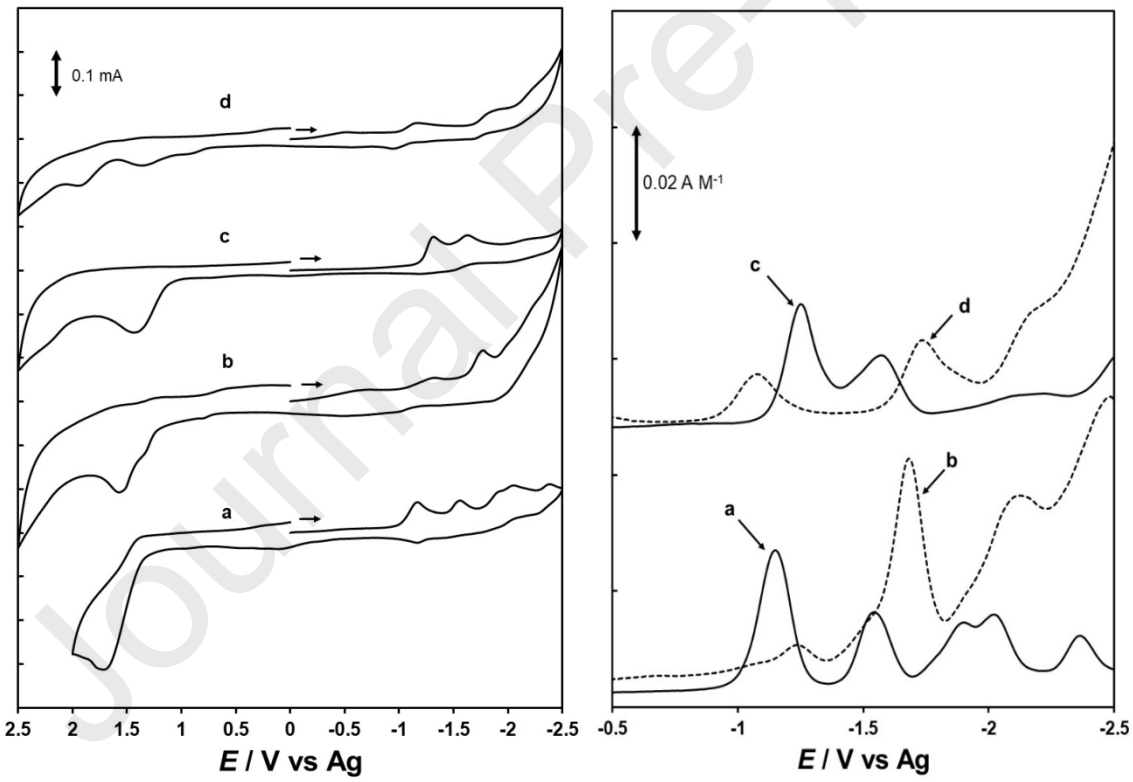

Figure 3. Left: Cyclic voltammograms of (a) 3.3 mM *pcta* in DMF[§], (b) = 2.6 mM **2**, (c) 3.0 mM *pdcta*, (d) 2.4 mM **1** in CH_3CN on a glassy carbon working electrode. Supporting electrolyte = 0.1

[§] The molecule pcta is sparingly soluble in CH_3CN.

M [^{n}Bu$_4$N]PF$_6$, scan rate = 200 mV s^{-1}. Right: Normalized (*I*/conc) squarewave voltammograms of the solutions given on the left hand side of the figure (squarewave frequency = 10 Hz).

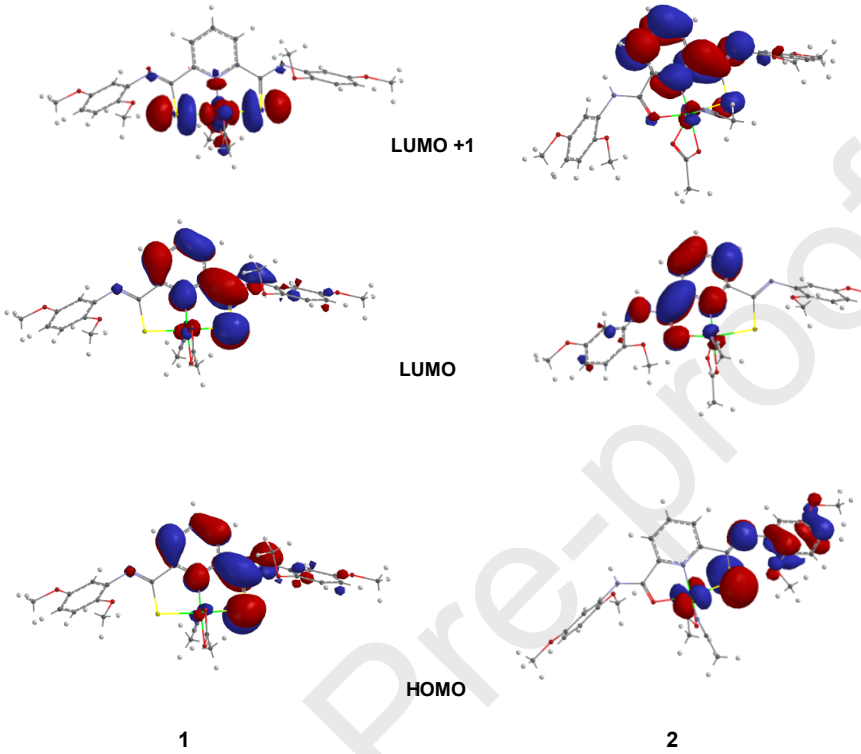

Figure 4. MOs of **1** and **2** calculated at the B3LYP/6-31G(d,p) level optimized in the gas phase.

3.2.1 Effect of co-ligands 2,2'-bipyridine and triphenyl phosphine on the voltammetric behaviour of 1 and 2

The presence of an exchangeable solvent molecule in the coordination sphere, along with the fairly labile solvent and acetate ligands on the Co(II) metal centre, led us to investigate the effect of a strongly coordinating ligands 2,2'-bipyridine (*bpy*) and triphenylphosphine (PPh_3) on the voltammetric response of complexes **1** and **2**. The ligands *bpy* and PPh_3 are known to impart favourable electrochemical properties on various metal centres, such as improving the reversibility of various oxidation states, altering the redox potentials, and providing steric bulk to improve the stability of reduced states [24, 38, 42, 55, 64, 75, 76]. The effects of the concentrations of PPh_3 and *bpy* on the $E_{1/2}$ values and the $i_{p,c}$ of the Co(II/I) redox couples of **1** and **2** are demonstrated in the Electronic Supporting Information (Section B). Voltammograms on CH_3CN solutions of **1** and **2** containing one equivalent of *bpy* showed shifts in the reduction potentials assigned to the metal

centres (Fig. 5, Table 2), as well as the removal of the adsorption wave occurred in its absence or its presence with complex and PPh_3 mixtures. The addition of one equivalent of *bpy* to **1** resulted in the $Co^{2+} \rightarrow Co^{+}$ reduction shifting from $E_{½}$ = –1.08 to –1.03 V, the $Co^{+} \rightarrow Co^{0}$ shifting to –1.74 to –1.67 V, and the $Co^{2+} \rightarrow Co^{3+}$ oxidation shifted from E_{pa} = +1.05 to to $E_{½}$ = +0.48 V (see Fig. 4). In complex **2**, the addition of one equivalent of *bpy* resulted in the $Co^{2+} \rightarrow Co^{+}$ reduction shifting from $E_{½}$ = –1.25 to –1.01 V. The $Co^{+} \rightarrow Co^{0}$ is resolved from the ligand reduction wave, and is observed at E_{pc} = –1.32 V. The $Co^{2+} \rightarrow Co^{3+}$ oxidation of **2** is also clearly resolved from ligand oxidation and is observed at $E_{½}$ = +0.44 V. The addition of *bpy* resulted in the Co(II/I) reduction potentials of both **1** and **2** becoming more positive by an average of 190 mV. The *bpy* co-ligand also shifted the $Co^{III/I}$ waves closer to zero by about 500 mV on average. The addition of PPh_3 resulted in the intermediate shift (relative to *bpy*) in the $Co^{II/I}$ redox process for both **1** and **2**. In the case of **1**, the reduction also become more Nernstian in behaviour (see Table 1), via the decrease in ΔE_p, and an increase in I_{pa}/I_{pc}. The $Co^{I/0}$ reduction is observed at –1.72 V in **1**, and appears at –1.49 V as a shoulder on the ligand reduction in **2**. The PPh_3 co-ligand had a marginal effect on the $Co^{2+} \rightarrow Co^{3+}$ oxidation potential which occurred at E_{pa} = +1.32 and +1.24 V for **1** and **2**, respectively. Although our primary interest is the Co(I) oxidation state, the dramatic shift induced by the *bpy* co-ligand on the $Co^{II/III}$ redox potentials was surprising. Also, the large and positive values of the $Co^{II/III}$ redox potential confirmed the remarkable stability of **1** and **2** towards aerobic oxidation.

Table 2. Effect of co-ligand on the reduction properties of the $Co^{2+} \rightarrow Co^{+}$ in CH_3CN (0.1 M $[^nBu_4N]PF_6$).

Complex	$E_{1/2}$ / V	I_{pa}/I_{pc}	ΔE_p / mV
1	–1.08	0.75	260
1/*bpy*	–1.03	0.80	150
1/PPh_3	–1.00	0.83	130
2	–1.23	0.61	150
2/*bpy*	–1.01	0.70	250
2/PPh_3	–1.17	0.60	170

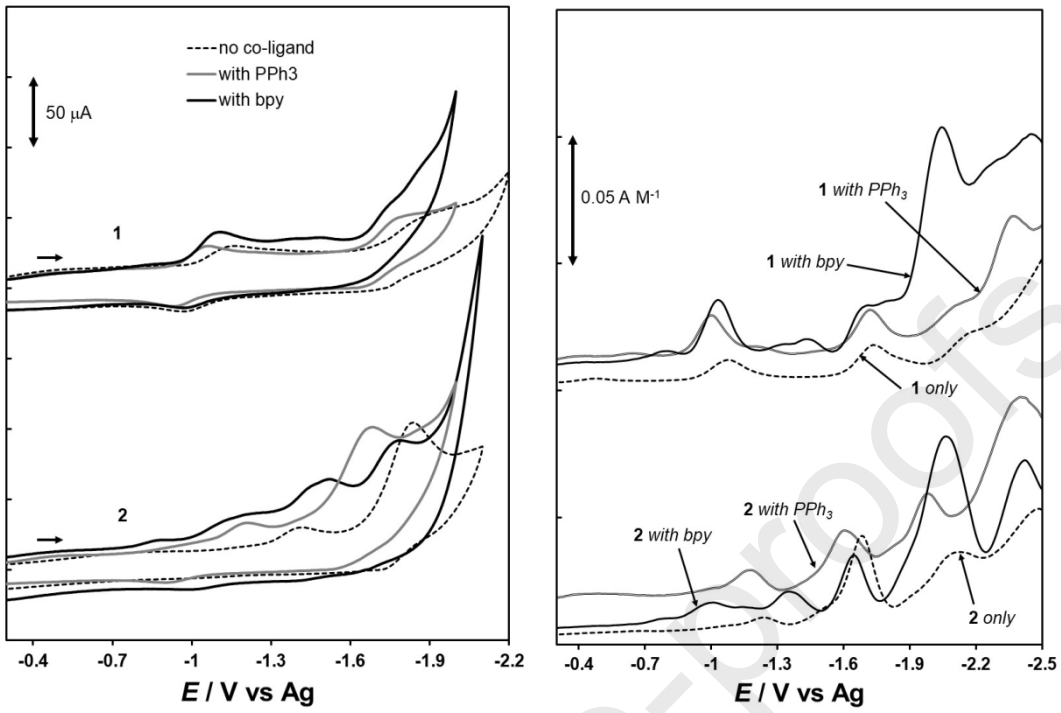

Figure 5. The effect of *bpy* and PPh_3 on the voltammograms (cyclic (left) at scan rate = 200 mV s^{-1} and (normalized as *I*/conc) square wave (right) at SW frequency = 10 Hz) of **1** and **2** in CH_3CN on a glassy carbon working electrode. Supporting electrolyte = 0.1 M $[^nBu_4N]PF_6$.

The stability of the Co(I) species is of interest in the application of Co-containing complexes as electro- or photo-catalytic species. In both complexes, the $Co^{2+} \rightarrow Co^{+}$ reduction has a quasi-reversible nature. The formation of Co(I) was examined by spectroelectrochemical methods. The spectral changes of **1** upon reduction at a constant potential of –1.1 V vs Ag is shown in Fig. S11. Upon reduction, the band at ca 300 nm is transformed into a shoulder on the MLCT band at 200 nm, and simultaneously, the intensity of the charge transfer band increases. Tetra-n-butyl borohydride ($[^nBu_4N]BH_4$) reduction of transition metals is also ubiquitous, and coordination complexes of Co(II) can be conveniently reduced to Co(I) state using the borohydride anion [41, 42]. The reduction of **1** and **2** with $[^nBu_4N]BH_4$ resulted in similar spectral transformations as those obtained via spectroelectrochemical methods, further suggesting that the spectral transformation was indeed that of the corresponding Co(I) species, and hence supports the $Co^{II/I}$ assignments in the voltammograms.

3.3 Electrochemical behaviour of 1 and 2 in the presence of *p*-toluene sulfonic acid monohydrate

Numerous cobalt-containing species have been associated with the electrocatalytic reduction of protons [11, 12, 41, 42, 77, 78]. The electrochemical behaviour of both complexes was investigated for electrocatalytic activity in the presence of *p*-toluene sulfonic acid (*p*-TSOH) as a proton source. In the presence of the proton source, both species showed a new cathodic wave within the vicinity of the Co(II/I) reduction wave (e.g., Fig. 6). This new wave was scan rate dependent (Fig. S12) and also increased with the concentration of *p*-TSOH. The electrocatalytic behaviour was also investigated with the *bpy* and PPh_3 co-ligands. In the absence of the co-ligands, both **1** and **2** exhibited a pre-wave in the vicinity of the adsorption wave observed in the absence of the proton source, and also an unexpected symmetrical peak on the return scan. This feature was only observed in the voltammograms with *p*-TSOH, at its variation with scan rate and [*p*-TSOH], and is suggestive of a stripping wave of the Co^0 from the electrode. In the presence of *bpy* and *p*-TSOH, complex **1** produced irreproducible voltammograms on consecutive cycling, and thus required cleaning of the electrode between acquisitions of each voltammogram. This is suggestive of modification or passivation of the electrode during electro-catalysis by a non-catalytic species [79-81], as rinsing the electrode and repeating the experiment resulted in diminished currents on each cycle. In the **1**/PPh_3/*p*-TSOH mixture, normal catalytic response was observed with successive additions of *p*-TSOH. On the other hand, the addition of *p*-TSOH to complex **2** resulted in cyclic voltammograms which displayed a pre-wave as well as an unexpected diffusional wave on the return scan, following the electrocatalytic wave. However, in the **2**/*bpy*/*p*-TSOH mixture, normal catalytic responses were observed (Fig. S13). Interestingly, in the **2**/PPh_3/*p*-TSOH mixture, normal catalytic response was observed at low [*p*-TSOH], and hysteresis was observed in the higher [*p*-TSOH]. Thus, the apparent catalytic response of **1** is improved with PPh_3, and **2** is improved with *bpy*.

Further studies on the electrocatalytic activity of the complexes were carried out by controlled potential electrolysis (CPE) of CH_3CN solutions of the complexes (with and without co-ligands) in the presence of *p*-TSOH. A CPE experiment on complex **1**, without co-ligands, at –1.1 V versus Ag, when corrected for a catalyst-free solution under the same potential, produced a net charge of 1.237 C after 1000 s of electrolysis, with accompanying evolution H_2 gas. A similar experiment on complex **2** at –1.25 V vs Ag gave a net charge of 0.828 C. The net volume of H_2

evolved correspond to 88 and 44 μL, representing 56 and 41% Faradaic efficiency for complexes **1** and **2**, respectively. In the presence of the co-ligands, CPE experiments at –0.90 V with *bpy* and –1.0 V with PPh_3, netted remarkably improved Faradaic efficiencies with **1**/PPh_3 compared to the marginal gain obtained in the **2**/*bpy* mixture (Table 3). The overpotential associated with the catalysed proton reductions (Eq. 2[**]) [82, 83] varied between the complexes and amongst the co-ligands. The results suggest that the *bpy* ligand has a positive effect on the Faradaic efficiency of the electrocatalytic response of **2**, however it has a negative effect on **1** in CH_3CN, whereas PPh_3 had a positive effect on **1** but an adverse effect on **2** (Table 3). The magnitude of the Gibbs free energy for the homolytic and heterolytic H_2 evolution from *p*-toluenesulfonic acid monohydrate (*p*-TSOH) in CH_3CN can be determined using the methodology suggested by Kellett and Spiro [43], on the basis of the values for the potentials of the cobalt and *p*-TSOH/H_2 couples versus Fc^+/Fc. In the analyses, it is evident that the thermodynamics of the hydrogen evolution tends to favour the homolytic pathway [35, 37], except in the **1**/*bpy* and **1**/PPh_3 systems. In the **1**/PPh_3 system, where both pathways are differentiated by ca. 14 kJ/mol, the highest Faradaic efficiency was obtained. Similarly, the **2**/bpy system, which possessed the smallest separation in energy for the competing pathways with pre-catalyst **2** (ca 27 kJ/mol), yielded the greatest Faradaic efficiency for pre-catalyst **2**. The turnover frequency (TOF) followed the trend *bpy* > no coligand > PPh_3 in both complexes. It is clear that the steric bulk retarded the hydrogen evolution, which supports a general preference for a homolytic pathway suggested by the thermodynamic analysis. The Faradaic efficiencies obtained are comparable to some Pd(II)-hydrazonic derivatives reported recently [84]. These results seem favourable when compared to cobalt complexes with [14]-tetraene-N4 (Tim) ligands of the type $[Co(Tim^{Ph/Me})X_2]^{n+}$ (X = Br or CH_3CN; n = 1 with X = Br and n = 3 with X = CH_3CN) which yielded 20-25% Faradaic efficiency [16]. However the **1**/PPh_3 system with its almost quantitative efficiency is comparable to some cobalt diglyoxime complexes in CH_3CN [16].

[**] where $\eta_{cat/2}$ is overpotential at the catalytic half-wave potential, $E°_{HA}$ (–0.65 V vs Fc^+/Fc [82] G.A.N. Felton, R.S. Glass, D.L. Lichtenberger, D.H. Evans, Inorg. Chem., 45 (2006) 9181-9184.doi:10.1021/ic060984e) is the reduction potential of *p*-TSOH in CH_3CN, pK_a of *p*-TSOH (8.7 [82] ibid.) in CH_3CN and $E_{cat/2}$ is determined from $Co^{II/I}$ in the presence *p*-TSOH *vs* Fc^+/Fc using square wave voltammetry.

$$\eta_{cat/2} = E^{\circ}_{HA} - E_{cat/2} \quad (2)$$

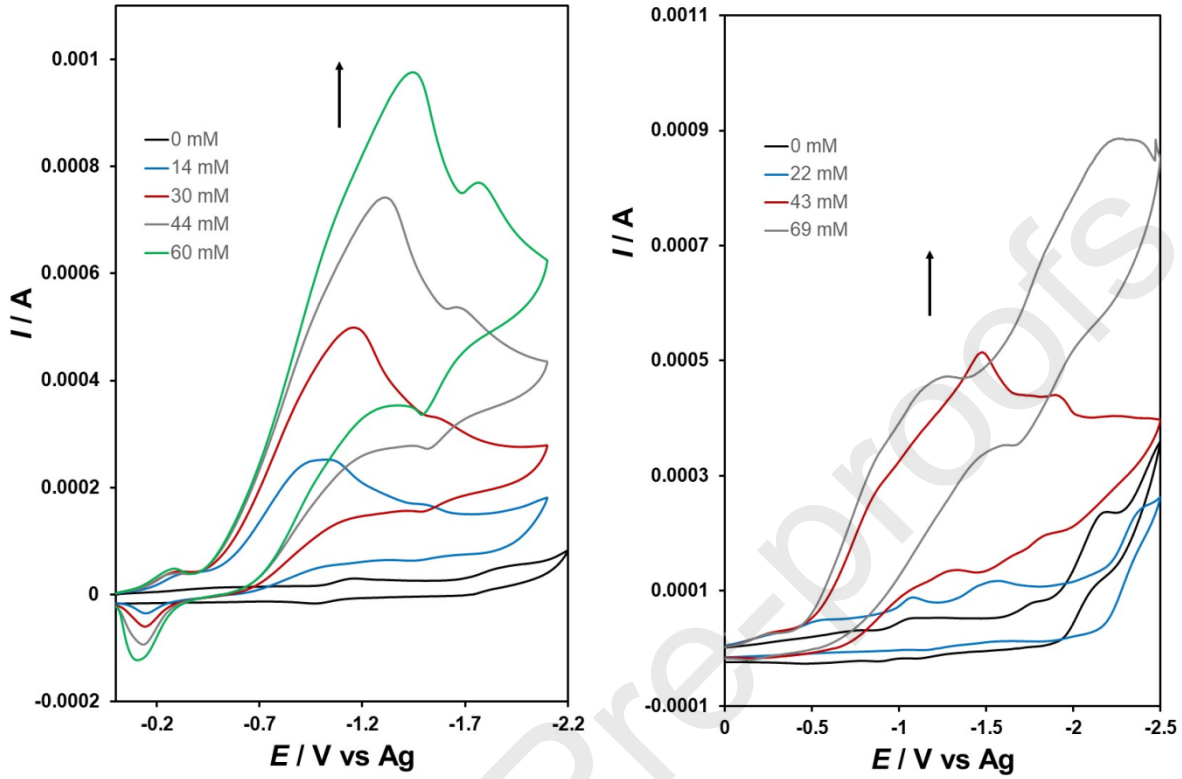

Figure 6. Cyclic voltammograms of **1** (left) and **1**/*bpy* (right) in the presence of varying quantities *p*-toluenesulfonic acid monohydrate (*p*-TSOH), at a glassy carbon working electrode in CH_3CN. [**1**] = 1.2 mM, [**1**/*bpy*] = 1.4 mM, supporting electrolyte = 0.1 M [^{n}Bu$_4$N]PF$_6$, scan rate = 200 mV s^{-1}.

Table 3. Effect of the co-ligands *bpy* and PPh_3 on the overpotential, Faradaic efficiency, turn over frequency, and free energy of the catalysed proton reduction of *p*-TSOH in CH_3CN.

Complex	$\eta_{cat/2}$/ mV	Faradaic efficiency / %	TOF / $\left(\frac{\mu mol\ H_2}{\mu mol\ cat} hr^{-1}\right)$	ΔG / kJ mol^{-1} (heterolytic pathway)	ΔG / kJ mol^{-1} (homolytic pathway)
1	750	56	5.5	–15.0	–87.8
1/*bpy*	650	51	6.2	–101	–83.0
1/PPh_3	680	97	2.2	–93.6	–80.0
2	780	41	2.1	–20.3	–101
2/*bpy*	605	44	3.0	–53.1	–81.0
2/PPh_3	780	40	0.93	–16.9	–102

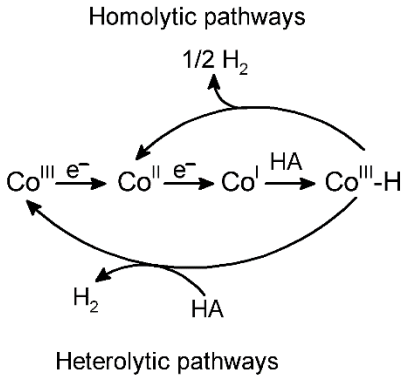

Scheme 4. Hydrogen evolution pathways from Co(I) intermediate[35, 43]. Ligands are excluded for clarity.

4 Conclusions

Two pincer Co(II) complexes of the type κ^3-SNS and ONS were synthesized. Both complexes displayed electrocatalytic hydrogen evolution in the presence and absence of *bpy* or PPh_3 co-ligands. The hydrogen evolution occurred at moderate overpotentials with the κ^3-SNS complex giving better Faradaic efficiencies than the κ^3-ONS under all the conditions explored. Further studies are in progress to isolate these and other mixed ligand systems in order to assess their potency in the hydrogen evolution reaction.

Acknowledgements

The authors are grateful for the kind assistance of the Department of Chemistry at The University of the West Indies, Mona and The University of Technology Jamaica for financial support. AAH would like to thank the National Science Foundation (NSF) for the NSF CAREER Award, as this material is based upon work supported by the NSF under CHE-1431172 (Formerly CHE-1151832). AAH would also like to thank Old Dominion University's Faculty Proposal Preparation Program (FP3). The authors are also grateful for the suggestions made by the reviewers.

References

[1] S.A. Asongu, S. Le Roux, N. Biekpe, Energy Policy, 111 (2017) 353-361.doi:https://doi.org/10.1016/j.enpol.2017.09.049
[2] J.-K. He, Advances in Climate Change Research, 7 (2016) 204-212.doi:https://doi.org/10.1016/j.accre.2016.06.007
[3] B. Tranberg, O. Corradi, B. Lajoie, T. Gibon, I. Staffell, G.B. Andresen, arXiv.org, e-Print Arch., Phys., (2018) 1-20

[4] A. Munir, K.S. Joya, T. Ul haq, N.-U.-A. Babar, S.Z. Hussain, A. Qurashi, N. Ullah, I. Hussain, ChemSusChem, 12 (2019) 1517-1548.doi:10.1002/cssc.201802069
[5] N. Armaroli, V. Balzani, Angew. Chem. Int. Ed., 46 (2007) 52-66.doi:10.1002/anie.200602373
[6] R. Eisenberg, D.G. Nocera, Inorg. Chem., 44 (2005) 6799-6801.doi:10.1021/ic058006i
[7] H.B. Gray, Nat. Chem., 1 (2009) 7-7.doi:10.1038/nchem.141
[8] M.I. Hoffert, K. Caldeira, A.K. Jain, E.F. Haites, L.D.D. Harvey, S.D. Potter, M.E. Schlesinger, S.H. Schneider, R.G. Watts, T.M.L. Wigley, D.J. Wuebbles, Nature, 395 (1998) 881-884.doi:10.1038/27638
[9] W. Lubitz, W. Tumas, Chem. Rev. , 107 (2007) 3900-3903
[10] R.F. Service, Science, 309 (2005) 548.doi:10.1126/science.309.5734.548
[11] M. Bacchi, G. Berggren, J. Niklas, E. Veinberg, M.W. Mara, M.L. Shelby, O.G. Poluektov, L.X. Chen, D.M. Tiede, C. Cavazza, M.J. Field, M. Fontecave, V. Artero, Inorg. Chem., 53 (2014) 8071-8082.doi:10.1021/ic501014c
[12] J.P. Bigi, T.E. Hanna, W.H. Harman, A. Chang, C.J. Chang, Chem. Commun., 46 (2010) 958-960.doi:10.1039/B915846D
[13] S. Carli, E. Busatto, S. Caramori, R. Boaretto, R. Argazzi, C.J. Timpson, C.A. Bignozzi, J. Phys. Chem. C, 117 (2013) 5142-5153.doi:10.1021/jp312066n
[14] A. Fihri, V. Artero, A. Pereira, M. Fontecave, Dalton Trans., (2008) 5567-5569
[15] A. Han, H. Wu, Z. Sun, H. Jia, Z. Yan, H. Ma, X. Liu, P. Du, ACS Applied Materials & Interfaces, 6 (2014) 10929-10934.doi:10.1021/am500830z
[16] X. Hu, B.S. Brunschwig, J.C. Peters, J. Am. Chem. Soc., 129 (2007) 8988-8998.doi:10.1021/ja067876b
[17] P.A. Jacques, V. Artero, J. Pecaut, M. Fontecave, Proc. Natl. Acad. Sci. USA, 106 (2009) 20627-20632.doi:10.1073/pnas.0907775106
[18] C.C.L. McCrory, C. Uyeda, J.C. Peters, J. Am. Chem. Soc., 134 (2012) 3164-3170.doi:10.1021/ja210661k
[19] W.R. McNamara, Z. Han, C.-J. Yin, W.W. Brennessel, P.L. Hollan, R. Eisenberg, Proc. Natl. Acad. Sci. USA, 109 (2012) 15594–15599.doi:10.1073/pnas.1120757109/-/DCSupplemental
[20] O. Pantani, E. Anxolabéhère-Mallart, A. Aukauloo, P. Millet, Electrochem. Commun., 9 (2007) 54-58.doi:10.1016/j.elecom.2006.08.036
[21] M. Shamsipur, A. Salimi, H. Haddadzadeh, M.F. Mousavi, J. Electroanal. Chem., 517 (2001) 37-44.doi:10.1016/S0022-0728(01)00644-1
[22] B.D. Stubbert, J.C. Peters, H.B. Gray, J. Am. Chem. Soc., 133 (2011) 18070-18073.doi:10.1021/ja2078015
[23] S. Varma, C.E. Castillo, T. Stoll, J. Fortage, A.G. Blackman, F. Molton, A. Deronzier, M.N. Collomb, Phys. Chem. Chem. Phys., 15 (2013) 17544-17552.doi:10.1039/c3cp52641k
[24] P. Zhang, P.-A. Jacques, M. Chavarot-Kerlidou, M. Wang, L. Sun, M. Fontecave, V. Artero, Inorg. Chem., 51 (2012) 2115-2120.doi:10.1021/ic2019132
[25] P. Zhang, M. Wang, J. Dong, X. Li, F. Wang, L. Wu, L. Sun, J. Phys. Chem. C, 114 (2010) 15868-15874.doi:10.1021/jp106512a
[26] Z. Kap, E. Ulker, S.V.K. Nune, F. Karadas, J. Appl. Electrochem., 48 (2018) 201-209.doi:10.1007/s10800-018-1152-z
[27] M. Kiker, A. Graves, W. Eckenhoff, Nickel Schiff base complexes for light driven H2 production, American Chemical Society, 2018, pp. INOR-361.
[28] S. Schnidrig, C. Bachmann, P. Mueller, N. Weder, B. Spingler, E. Joliat-Wick, M. Mosberger, J. Windisch, R. Alberto, B. Probst, ChemSusChem, 10 (2017) 4570-4580.doi:10.1002/cssc.201701511
[29] S. Xi, J. Tubb, T. Liu, W. McNamara, Iron complexes containing pendant amines for hydrogen generation, American Chemical Society, 2017, pp. CHED-240.
[30] C. Baffert, V. Artero, M. Fontecave, Inorg. Chem., 46 (2007) 1817-1824.doi:10.1021/ic061625m
[31] P. Connolly, J.H. Espenson, Inorg. Chem., 25 (1986) 2684-2688.doi:10.1021/ic00236a006
[32] A. Fihri, V. Artero, M. Razavet, C. Baffert, W. Leibl, M. Fontecave, Angew. Chem. Int. Ed. , 47 (2008) 564-567

[33] D.M. Cropek, A. Metz, A.M. Muller, H.B. Gray, T. Horne, D.C. Horton, O. Poluektov, D.M. Tiede, R.T. Weber, W.L. Jarrett, J.D. Phillips, A.A. Holder, Dalton Trans., 41 (2012) 13060-13073
[34] Q.-X. Peng, L.-Z. Tang, S.-T. Ren, L.-P. Ye, Y.-F. Deng, S.-Z. Zhan, Chemical Physics Letters, 662 (2016) 152-155.doi:https://doi.org/10.1016/j.cplett.2016.09.017
[35] J.L. Dempsey, B.S. Brunschwig, J.R. Winkler, H.B. Gray, Acc. Chem. Res., 42 (2009) 1995-2004
[36] S.C. Marinescu, J.R. Winkler, H.B. Gray, Proc. Natl. Acad. Sci. USA, 109 (2012) 15127-15131.doi:10.1073/pnas.1213442109
[37] J.L. Dempsey, J.R. Winkler, H.B. Gray, J. Am. Chem. Soc., 132 (2010) 1060–1065
[38] C. Creutz, N. Sutin, Coord. Chem. Rev., 64 (1985) 321-341.doi:10.1016/0010-8545(85)80058-8
[39] D.P. Estes, D.C. Grills, J.R. Norton, J. Am. Chem. Soc., 136 (2014) 17362-17365.doi:10.1021/ja508200g
[40] G.N. Glavee, K.J. Klabunde, C.M. Sorensen, G.C. Hadjipanayis, Inorg. Chem., 32 (1993) 474-477.doi:10.1021/ic00056a022
[41] M.A.W. Lawrence, M.J. Celestine, E.T. Artis, L.S. Joseph, D.L. Esquivel, A.J. Ledbetter, D.M. Cropek, W.L. Jarrett, C.A. Bayse, M.I. Brewer, A.A. Holder, Dalton Trans., 45 (2016) 10326-10342.doi:10.1039/C6DT01583B
[42] M.A.W. Lawrence, A.A. Holder, Inorg. Chim. Acta, 441 (2016) 157-168.doi:10.1016/j.ica.2015.11.016
[43] R.M. Kellett, T.G. Spiro, Inorg. Chem., 24 (1985) 2373-2377.doi:10.1021/ic00209a011
[44] S. Shi, L.M. Daniels, J.H. Espenson, Inorg. Chem., 30 (1991) 3407-3410.doi:10.1021/ic00018a008
[45] D.P. Hickey, C. Sandford, Z. Rhodes, T. Gensch, L.R. Fries, M.S. Sigman, S.D. Minteer, J. Am. Chem. Soc., 141 (2019) 1382-1392.doi:10.1021/jacs.8b12634
[46] T.L.C. Green, P.N. Nelson, M.A.W. Lawrence, J. Mol. Struct., 1195 (2019) 426-434.doi:10.1016/j.molstruc.2019.06.011
[47] O.R. Luca, J.D. Blakemore, S.J. Konezny, J.M. Praetorius, T.J. Schmeier, G.B. Hunsinger, V.S. Batista, G.W. Brudvig, N. Hazari, R.H. Crabtree, Inorg. Chem., 51 (2012) 8704-8709.doi:10.1021/ic300009a
[48] O.R. Luca, S.J. Konezny, J.D. Blakemore, D.M. Colosi, S. Saha, G.W. Brudvig, V.S. Batista, R.H. Crabtree, New J. Chem., 36 (2012) 1149-1152.doi:10.1039/C2NJ20912H
[49] P. Sponholz, D. Mellmann, C. Cordes, P.G. Alsabeh, B. Li, Y. Li, M. Nielsen, H. Junge, P. Dixneuf, M. Beller, ChemSusChem, 7 (2014) 2419-2422.doi:10.1002/cssc.201402426
[50] D.S. Marlin, M.M. Olmstead, P.K. Mascharak, Inorg. Chem., 40 (2001) 7003-7008.doi:10.1021/ic010523n
[51] M.A.W. Lawrence, Y.A. Jackson, W.H. Mulder, P.M. Björemark, M. Håkansson, Aust. J. Chem., 68 (2015) 731-741.doi:10.1071/CH14380
[52] R.A. Begum, D. Powell, K. Bowman-James, Inorg. Chem., 45 (2006) 964-966.doi:10.1021/ic051775h
[53] T.-a. Koizumi, T. Teratani, K. Okamoto, T. Yamamoto, Y. Shimoi, T. Kanbara, Inorg. Chim. Acta, 363 (2010) 2474-2480.doi:10.1016/j.ica.2010.04.012
[54] T. Teratani, T.-a. Koizumi, T. Yamamoto, K. Tanakab, T. Kanbara, Dalton Trans., 40 (2011) 8879-8886.doi:10.1039/c0dt01283a
[55] Y. Komiyama, J. Kuwabara, T. Kanbara, Organometallics, 33 (2014) 885-891.doi:10.1021/om400969p
[56] Q.Q. Wang, R.A. Begum, V.W. Day, K. Bowman-James, Inorg. Chem., 51 (2012) 760-762.doi:10.1021/ic202087u
[57] M.A.W. Lawrence, W.H. Mulder, ChemistrySelect, 3 (2018) 8387-8394.doi:10.1002/slct.201802065
[58] M. Bakir, M.A.W. Lawrence, S. McBean, Spectrochim. Acta, Part A, 146 (2015) 323-330.doi:10.1016/j.saa.2015.03.079
[59] M. Bakir, M.A.W. Lawrence, M. Singh-Wilmot, J. Coord. Chem., 60 (2007) 2385-2399.doi:10.1080/00958970701266732
[60] M.A.W. Lawrence, P.T. Maragh, T.P. Dasgupta, J. Coord. Chem., 63 (2010) 2517-2527.doi:10.1080/00958972.2010.491546

[61] M.A.W. Lawrence, P.T. Maragh, T.P. Dasgupta, Inorg. Chim. Acta, 388 (2012) 88-97.doi:10.1016/j.ica.2012.02.038
[62] M.A.W. Lawrence, P.T. Maragh, T.P. Dasgupta, Transition Met. Chem., 37 (2012) 505-517.doi:10.1007/s11243-012-9616-1
[63] M.A.W. Lawrence, S.E. Thomas, P.T. Maragh, T.P. Dasgupta, Transition Met. Chem., 36 (2011) 553-563.doi:10.1007/s11243-011-9502-2
[64] M.A.W. Lawrence, C.D. McMillen, R.K. Gurung, M.J. Celestine, J.F. Arca, A.A. Holder, J Chem Crystallogr, 45 (2015) 427-433.doi:10.1007/s10870-015-0610-2
[65] M. Bakir, M.A.W. Lawrence, P.N. Nelson, R.R. Conry, Electrochim. Acta, 212 (2016) 1010-1020.doi:10.1016/j.electacta.2016.07.051
[66] M. Bakir, M.A.W. Lawrence, M. Ferhat, R.R. Conry, J. Coord. Chem., 70 (2017) 3048-3064.doi:10.1080/00958972.2017.1374379
[67] W.L.F. Armarego, C.L.L. Chai, Chapter 4 - Purification of Organic Chemicals, Purification of Laboratory Chemicals (Fifth Edition), Butterworth-Heinemann, Burlington, 2003, pp. 80-388.
[68] T. Fang, L.-Z. Fu, L.-L. Zhou, S.-Z. Zhan, S. Chen, Electrochim. Acta, 178 (2015) 368-373.doi:10.1016/j.electacta.2015.07.180
[69] M. Necki, M. Heliasz, J. Rosiek, M. Pycia, K. Rozanski, I. Sliwka, J. Bartyzel, Chem. Anal. (Warsaw), 54 (2009) 705-715
[70] M.S. Gordon, M.W. Schmidt, Chapter 41 - Advances in electronic structure theory: GAMESS a decade later, in: C.E. Dykstra, G. Frenking, K.S. Kim, G.E. Scuseria (Eds.) Theory and Applications of Computational Chemistry, Elsevier, Amsterdam, 2005, pp. 1167-1189.
[71] M.W. Schmidt, K.K. Baldridge, J.A. Boatz, S.T. Elbert, M.S. Gordon, J.H. Jensen, S. Koseki, N. Matsunaga, K.A. Nguyen, S. Su, T.L. Windus, M. Dupuis, J.A. Montgomery Jr, J. Comput. Chem., 14 (1993) 1347-1363.doi:10.1002/jcc.540141112
[72] M.D. Hanwell, D.E. Curtis, D.C. Lonie, T. Vandermeersch, E. Zurek, G.R. Hutchison, J. Cheminf., 4 (2012) 17.doi:10.1186/1758-2946-4-17
[73] G.M. Sheldrick, SHELXL 2014/7, University of Gottngen, Germany, 2014.
[74] O.M. Williams, A.H. Cowley, M.J. Rose, Dalton Trans., 44 (2015) 13017-13029.doi:10.1039/C5DT00924C
[75] S. Margel, W. Smith, F.C. Anson, J. Electrochem. Soc., 125 (1978) 241-246.doi:10.1149/1.2131421
[76] K.M. Kadish, W. Koh, P. Tagliatesta, D. Sazou, R. Paolesse, S. Licoccia, T. Boschi, Inorg. Chem., 31 (1992) 2305-2313.doi:10.1021/ic00038a005
[77] J.C. Manton, C. Long, J.G. Vos, M.T. Pryce, Dalton Trans., 43 (2014) 3576-3583.doi:10.1039/C3DT53166J
[78] M. Vennampalli, G. Liang, L. Katta, C.E. Webster, X. Zhao, Inorg. Chem., 53 (2014) 10094-10100.doi:10.1021/ic500840e
[79] J.-M. Savéant, Chem. Rev., 108 (2008) 2348-2378.doi:10.1021/cr068079z
[80] C. Costentin, J.-M. Savéant, ChemElectroChem, 1 (2014) 1226-1236.doi:10.1002/celc.201300263
[81] K.J. Lee, B.D. McCarthy, J.L. Dempsey, Chem. Soc. Rev., 48 (2019) 2927-2945.doi:10.1039/C8CS00851E
[82] G.A.N. Felton, R.S. Glass, D.L. Lichtenberger, D.H. Evans, Inorg. Chem., 45 (2006) 9181-9184.doi:10.1021/ic060984e
[83] E.S. Wiedner, R.M. Bullock, J. Am. Chem. Soc., 138 (2016) 8309-8318.doi:10.1021/jacs.6b04779
[84] M. Bakir, M.W. Lawrence, P. Nelson, M.B. Yamin, J. Coord. Chem., 72 (2019) 2261-2278.doi:10.1080/00958972.2019.1645329

Highlights:

- Two Co(II)-pincer ligands based on pyridyl(di)thiocarboamide of κ^3-SNS and κ^3-ONS are reported
- The crystal structure of *N*-(2,5- dimethoxyphenyl)-6-[(2,5-dimethoxyphenyl)carbamothioyl]pyridine-2-carboxamide (*pcta*) is reported
- Both complexes of Co(II) displayed electro-catalytic hydrogen evolution (HER)
- The addition of co-ligands *bpy* or PPh_3 had varying effects on the HER

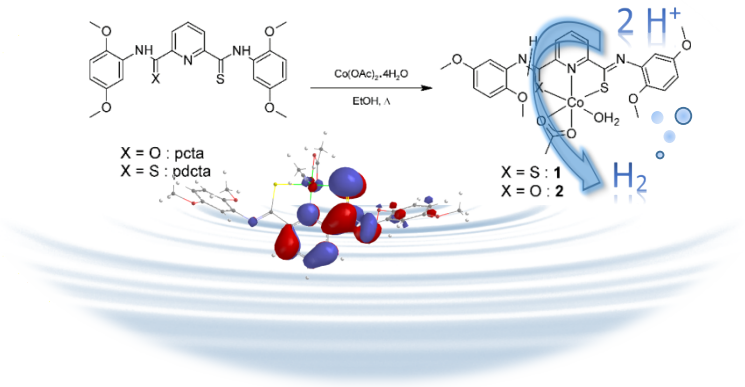

Author Statement

Mark A.W. Lawrence: Conceptualization, Methodology, Experimentation and Data processing, Initial draft preparation, Graphical Preparation, Reviewing, Editing.

Willem Mulder: Methodology, Data checking, Writing, Reviewing, Editing.

Michael J. Celestine: Experimentation, Data processing, Editing

Colin D. McMillen: Experimentation, X-ray structure solution, Writing, Reviewing, Editing

Alvin A. Holder: Writing, Reviewing, Editing